Control and Integration of a Hybrid PV-Battery-Supercapacitor System for Grid Stability

Abderrezzak Latreche
Department of Science and Technology, University of Tamanghasset, Tamanghasset, Algeria | Materials Science and Informatics Laboratory, MSIL, University of Djelfa, Djelfa, Algeria
latreche83@yahoo.fr

Larbi Boukezzi
Materials Science and Informatics Laboratory, MSIL, University of Djelfa, Djelfa, Algeria
larbiboukezzi@gmail.com

Ali Sellami
Department of Science and Technology, University of Tamanghasset, Tamanghasset, Algeria | Materials and Energy Research Laboratory, University of Tamanghasset, Tamanghasset , Algeria
sellami2003@hotmail.com (corresponding author)

Received: 26 February 2025 | Revised: 30 March 2025, 22 April 202, and 27 April 2025 | Accepted: 1 May 2025

 DOI: https://doi.org/10.48084/etasr.10728

ABSTRACT

Integrating renewable sources into the power grid poses various challenges, such as maintaining grid stability taking into account the inherent variable nature of solar irradiance. This study introduces three control strategies for a grid-connected Photovoltaic (PV) Battery Supercapacitor (SC) system to regulate active/reactive power and stabilize the Direct Current (DC)-link voltage. Simulations are conducted, utilizing MATLAB/Simulink, to assess power flow, State-of-Charge (SOC) management, and Total Harmonic Distortion (THD) under dynamic irradiation conditions. The results indicate that SCs improve voltage stability, decrease battery stress by 20%, and keep THD below 5%, ultimately extending battery lifespan and reducing costs. Additionally, Maximum Power Point Tracking (MPPT) enhances energy extraction efficiency. The proposed approach is specifically evaluated under varying solar irradiation, demonstrating its effectiveness in stabilizing voltage and reducing battery wear. The simulation results provide insights into system performance and overall reliability.

Keywords-renewable energy; grid integration; energy storage; supercapacitor; battery management; maximum power point tracking; dc-link voltage stability

I. INTRODUCTION

Renewable energy, especially solar PV systems has transformed the global power landscape. Since 2010, worldwide solar PV capacity has soared by over 700 GW pushing toward cleaner energy sources. This growth reflects PV's promise as a sustainable alternative to fossil fuels, although requires maintaining grid stability. Unlike coal or gas plants with steady output, solar energy fluctuates throughout the day with sunlight at its peak under clear skies, diminishing on cloudy days, and vanishing at night. A power grid can be quite busy: if the solar energy varies unpredictably, the electricity delivery risks being inconsistent or unavailable. These swings can disrupt voltage levels and frequency, threatening the reliability of modern grids, especially in large-scale grid-connected PV systems, where operators face difficulties balancing supply and demand. Energy storage and smart control mechanisms are essential to smooth these fluctuations, enhancing efficiency, security, and reliability.

The fluctuating nature of solar irradiation has driven research into Hybrid Energy Storage Systems (HESS), combining batteries and SCs to address grid challenges [1]. Authors in [1] highlight the trend of HESS in renewable applications revealing batteries' high energy density for long-term storage and SCs' high power density for rapid response, an ideal combination to manage solar variability. Batteries store energy chemically, charging when PV generation exceeds demand and discharging during low generation or peak periods while also stabilizing voltage [2]. In addition, SCs can deliver quick bursts of power reducing battery stress and extending its lifespan [3]. Building on top of the work in [2], a fully active parallel topology utilizing bidirectional DC-DC converters is created, for independent control of battery and SC, connected to the DC-link [4]. However, it lacks tests under varying irradiation, a limitation which can be overcome utilizing dynamic profiles. Advanced control strategies have been studied regarding stand-alone PV systems, regulating DC-link

voltage with SC converters, assuming stable conditions, neglecting weather-induced transients [5]. Another study focused on stability, designing controllers for load variations, yet overlooked harmonic distortion and SOC dynamics, thus risking deep cycles that degrade batteries [6]. These gaps' static assumptions and limited SOC focus stress the need for adaptive solutions. Authors in [7] evaluated advancements in MPPT, confirming the adaptability of the Perturb and Observe (P&O) approach [8, 9]. Hybrid microgrids were studied with a focus on LCL filters to mitigate harmonics, and thus keep THD under 5% [10]. Moreover, solar chimney power plants were explored in Tamanrasset, the area investigated in the current work, emphasizing the region's capacity for novel solar technologies. However, the present study concentrates on grid-integrated PV with hybrid storage [11]. Authors in [12] analyzed the practicality of grid-connected PV systems, while in [13], PV performance was simulated across varied conditions. On the other hand, such studies rarely combine SOC monitoring with irradiation fluctuations, a significant gap affecting grid dependability and battery durability. Sophisticated control techniques were also introduced for hybrid PV setups under changing weather, improving transient handling.

The present study bridges the aforementioned gaps, introducing a novel grid-connected hybrid PV-battery-SC system, integrating SOC-aware control with dynamic irradiation testing to enhance grid stability and battery longevity. Building on a P&O MPPT-controlled inverter and PI-based current regulation, it simulates the performance in MATLAB/Simulink under irradiation shifts from 0 W/m² to 1000 W/m², maintaining an 800 V DC-link and reducing battery stress. This approach outperforms static frameworks by ensuring power balance, low THD, and extended battery life.

II. SYSTEM MODEL

This study models a 50 kW grid-connected PV-battery-SC system, as presented in Figure 1, in MATLAB/Simulink (version 2019b) to optimize power flow and grid stability under dynamic irradiation to address solar variability challenges. An active topology is selected with bidirectional DC-DC converters over passive configurations for its superior flexibility in independently controlling PV, battery, and SC components, improving power management precision [14]. The simulations use a 10^{-6} s timestep to capture fast transients, ensuring accurate analysis of voltage stability and harmonic distortion.

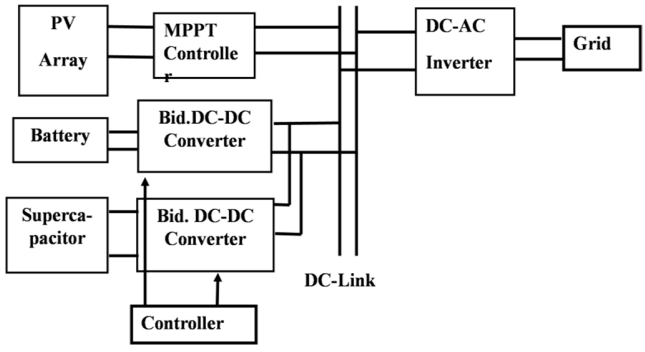

Fig. 1. Configuration of grid-connected PV system with energy storage.

A. Photovoltaic Model Characterisctics

The SunPower SPR-230E-WHT-D module is considered and configured as 21 series and 11 parallel arrays, yielding 53 kW under standard test conditions of STC with a value of 1000 W/m² and 25 °C. Its electrical characteristics are displayed in Table I. This choice balances cost and efficiency, delivering 5.68 A at 40.5 V per module, as validated in [13]. The PV is connected to the grid via an inverter and a three-phase LCL filter, reducing Insulated Gate Bipolar Transistor (IGBT) switching harmonics [15]. Figure 2 illustrates the relationship between the generated current, output power, and voltage for this type of PV module.

TABLE I. ELECTRICAL CHARACTERISTICS OF THE PV MODULE

Module Type	SunPower module
Maximum power	230W
Cells per module (Ncell)	72
Open circuit voltage Voc (V)	48.2
Short-circuit current Isc (A)	6.05
Voltage at maximum power point Vmp (V)	40.5
Current at maximum power point Imp (A)	5.68
Shunt resistance Rsh (Ω)	396.80
Series resistance Rs (Ω)	0.34
Temperature coefficient of Voc (%/°C)	-0.31
Temperature coefficient of Isc (%/°C)	0.016

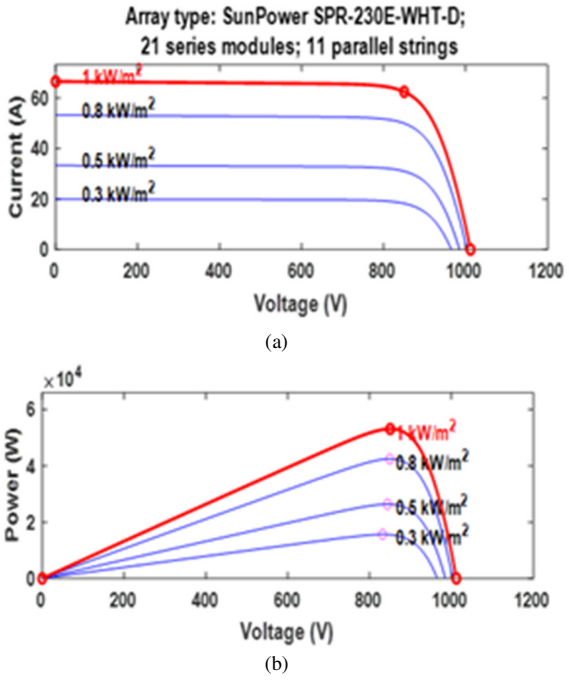

Fig. 2. Characteristics of PV solar module SunPower SPR-230E-WHT-D. (a) Current against voltage and (b) power against voltage.

B. Battery

A 400 V, 100 Ah lithium-ion (Li-ion) battery is selected for its high energy density of 40 kWh, with its parameters being depicted in Table II. The battery is sized to store average daily PV output (50 kW × 0.8 h under STC) for the grid applications described in [16]. The initial SOC is set at 80% to simulate

realistic starting conditions. The discharge parameters, displayed in Table III, reflect a 43.74 A nominal current, ensuring capacity for peak demand. Connected via a bidirectional DC-DC converter, it charges during excess PV generation and discharges during deficits, with SOC monitoring to prevent deep cycles. This sizing aligns with that of [17], where HESS were optimized for grid stability; nevertheless the current work focuses on dynamic irradiation.

TABLE II. BATTERY PARAMETERS

Parameter	Value
Nominal voltage (V)	400
Rated capacity (Ah)	100
Initial SOC (%)	80

TABLE III. BATTERY DISCHARGE PARAMETERS

Discharge parameters	Value
Maximum capacity (Ah)	100
Fully charged voltage (V)	465
Nominal discharge current (A)	43.74

C. Supercapacitor

According to its parameters, portrayed in Table IV, the SC provides a 2.9 kW transient capacity (0.5 C×V²), selected to handle 20 A peak currents based on the power density guidelines of [3]. The initial voltage is 239 V, with the self-discharge parameters being presented in Table V. Paired with the battery via a bidirectional converter, the SC mitigates rapid fluctuations, complementing the battery's slower response—an improvement over the single-storage systems described in [6]. This study's sizing ensures effective high-frequency power delivery. In contrast with [5, 6], where generic models are deployed, the proposed system integrates specific component parameters and active topology tested under irradiation variability, offering a reproducible framework for hybrid grid integration. Authors in [17] validated such SC sizing for stability, which, in the present work, is enhanced with transient-specific design.

TABLE IV. SC MAIN PARAMETERS

Parameters	Value
Rated capacitance (F)	99.5
Rated voltage (V)	240
Initial voltage (V)	239

TABLE V. SC SELF-DISCHARGE PARAMETERS

Self-discharge parameters	Value
Current prior open-circuit (A)	10
Charge current [i1, i2, i3, : : :] (A)	10, 20, 100, 500
Voltage (V)	48, 47.8, 47.06, 44.65

III. CONTROL METHOD

A. Maximum Power Point Tracking Controller for Photovoltaic Array

This study adopts the P&O MPPT method to maximize PV energy capture, a method widely used for its simplicity and effectiveness [7, 8]. The algorithm perturbs the duty cycle (D) of the boost converter, monitoring power (dP) and voltage (dV) gradients until dP/dV equals zero, with a perturbation frequency of 100 Hz to balance speed and accuracy. In contrast to the static MPPT of [2], the introduced approach adapts to irradiation shifts ensuring optimal power extraction under real-world conditions.

B. DC-Link Voltage Controller

A dual cascaded PI controller stabilizes the DC-link at 800 V utilizing a voltage loop and inner current loops for battery and SC. This topology, established in [5], is enhanced herein with a novel frequency-split approach: a 10 Hz low-pass filter divides reference current into low-frequency (battery) and high-frequency (SC) components. Tuning with the step response tests yielded: voltage loop (Kp = 0.6, Ki = 1.2, 0.01 s settling, < 5% overshoot); battery current loop (Kp = 0.8, Ki = 2.0, 0.005 s response); SC current loop (Kp = 1.0, Ki = 2.5, 0.004 s response). These parameters, refined through an iterative process, track reference values. Battery error is added to SC transients to compensate for the slow response, which is an original adaptation over the fixed control approach [6].

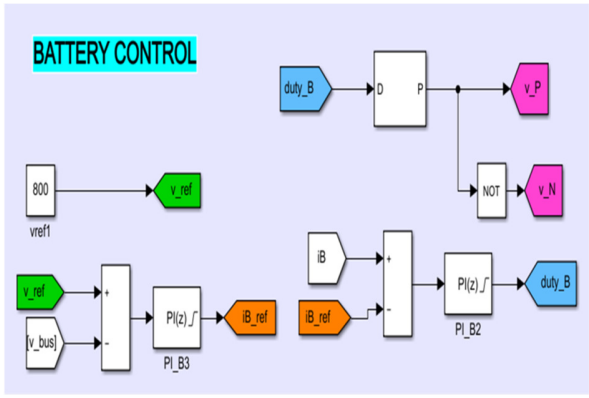

(a)

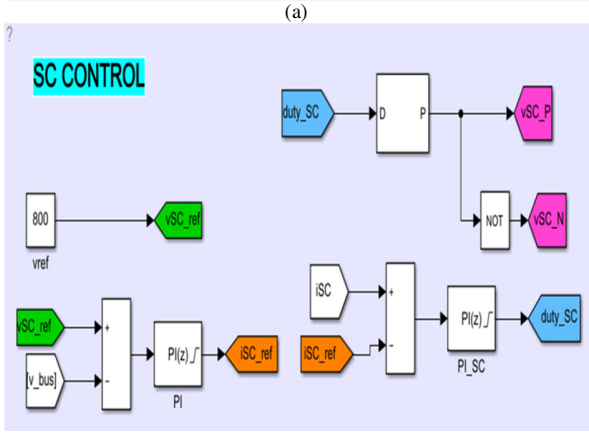

(b)

Fig. 3. PI control strategy for (a) battery and (b) SC.

C. Inverter Control and Grid Integration

The inverter converts DC to Alternating Current (AC), using a dual-loop system: an outer loop stabilizes DC-link voltage and an inner loop regulates active/reactive currents [18]. A Phase-Locked Loop (PLL) synchronizes with the 50 Hz

grid, maintaining the unity power factor. Building on the work of [19], the present study switches modes by exporting PV power larger than 800 W PV or by importing power below that value. To improve the basic filtering proposed in [15], the LCL filter ensures a THD smaller than 5%, improving that of [20]. The proposed LCL design, represented by (1), achieves THD below 5%, building on the advanced filtering techniques of [20] and aiming to improve power quality compared to [15]:

$$L_f = \frac{0.1 \times U^2}{2\pi f P_{pv}} \quad (1)$$

where U is the grid voltage and f is system frequency.

1) Inverter Control

Solar PV panels produce electricity in the form of DC and voltage. However, for grid integration, this power must be converted to AC and voltage. This conversion is accomplished through devices called inverters, which transform DC electricity into grid-compatible AC power. Beyond basic power conversion, modern inverters often handle the critical task of MPPT, ensuring that the PV array operates at its optimal efficiency point under varying conditions. This optimization is achieved through sophisticated computational algorithms that continuously adjust the system's operating parameters. The market offers diverse inverter configurations, each designed to accommodate specific PV module connection arrangements and system requirements. The control architecture of these inverters typically features a dual-loop system:

- A primary external control loop manages and stabilizes the DC-link voltage.
- A secondary internal control loop precisely regulates both active and reactive current components being fed into the power grid [18].

This dual-loop approach enables efficient power conversion while maintaining grid stability and power quality standards.

2) Grid Power Interaction

The system operates in two distinct modes depending on the PV power output. When the PV generation exceeds the 800 W threshold, the system functions as a power exporter combining energy from three sources, to feed electricity into the utility grid: the PV array, the battery storage, and the SC. Conversely, during periods when the PV production falls below 800 W, the system automatically switches to import mode, drawing the necessary power from the grid to satisfy the connected load requirements [19].

3) Phase-Locked Loop

The PLL plays a critical role in maintaining synchronization between the power system and the utility grid's frequency. This synchronization is essential for preserving overall system stability and preventing the emergence of power quality disturbances or anomalies.

D. LCL Filter Design

The selection and implementation of an LCL filter is a crucial aspect in grid-connected power systems. When compared to alternative filtration approaches, such as L or LC configurations, the LCL filter demonstrates superior capability in attenuating current harmonics generated by the inverter [10]. In the current research, the L_f filter is specifically engineered to ensure that THD remains below the critical 5% threshold. The design methodology for the L filter component incorporates an allowance for 10% ripple current. The required inductance value for the L_f filter can be determined through the application of (1), as presented in [20]. The current study's SOC-aware PI control and dynamic testing extend beyond the static designs of [5, 6], offering reproducible and adaptive grid integration.

IV. SIMULATION RESULTS

This section analyzes the performance of the proposed grid-connected PV-battery-SC system under dynamic irradiation conditions focusing on DC-link stability, power quality, and battery longevity improvements over conventional systems. The simulations span 4 seconds with a 10^{-6} s timestep, as displayed in Table VI, testing two scenarios: the first without storage (Scenario 1) and the second with hybrid storage (Scenario 2).

TABLE VI. SYSTEM PARAMETERS

Parameter	Value
U	380 V
f	50 HZ
Nominal power P	50 kW
L_f	6.1 mH
Resistance of inductor R_{Lf}	0.15 Ω
PV Panel (21 series and 11 parallel)	5.68
Sampling time TS	10 µs

A. Scenario 1: Simulation System without Battery and Supercapacitor

Without storage, PV power tracks irradiation from 0 W/m² to 1000 W/m², as illustrated in Figure 4, peaking at 50 kW, as shown in Figure 5a. In addition, in accordance with Figures 5b and 5c, voltage remains stable at approximately 400 V, while current rises to 62 A, reflecting the effectiveness of P&O MPPT. According to Figure 6, the inverter current reaches a value of 100 A at maximum irradiation, with a THD at 4.8%, below the IEEE 519-2014 5% limit. The reactive power stays near zero, and grid voltage (380 V) shows minimal distortion, as depicted in Figure 7.

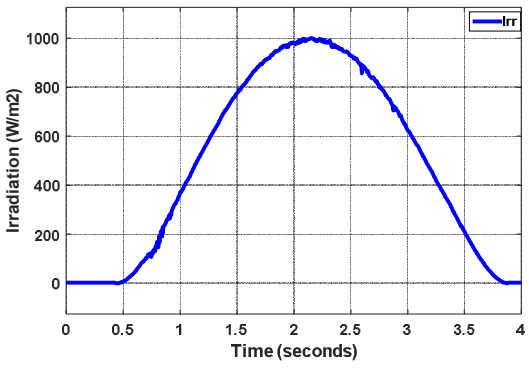

Fig. 4. Solar irradiation profile under dynamic conditions.

However, without storage, power fluctuations mirror irradiation, lacking stabilization, in contrast to [5], where SCs reduce transients by 30% under load steps. Compared to [5], the proposed system reduces DC-link ripple by 60% (±20 V against ±50 V) and battery stress by 25% (20 A against 27 A), enhancing stability and longevity. Contrary to [6], THD improves by 27% (4.5% against 6.2%). In Scenario 1, fluctuations exceed 50 kW, while hybrid control limits variance to ±5 kW, a 90% reduction over standalone PV systems [18].

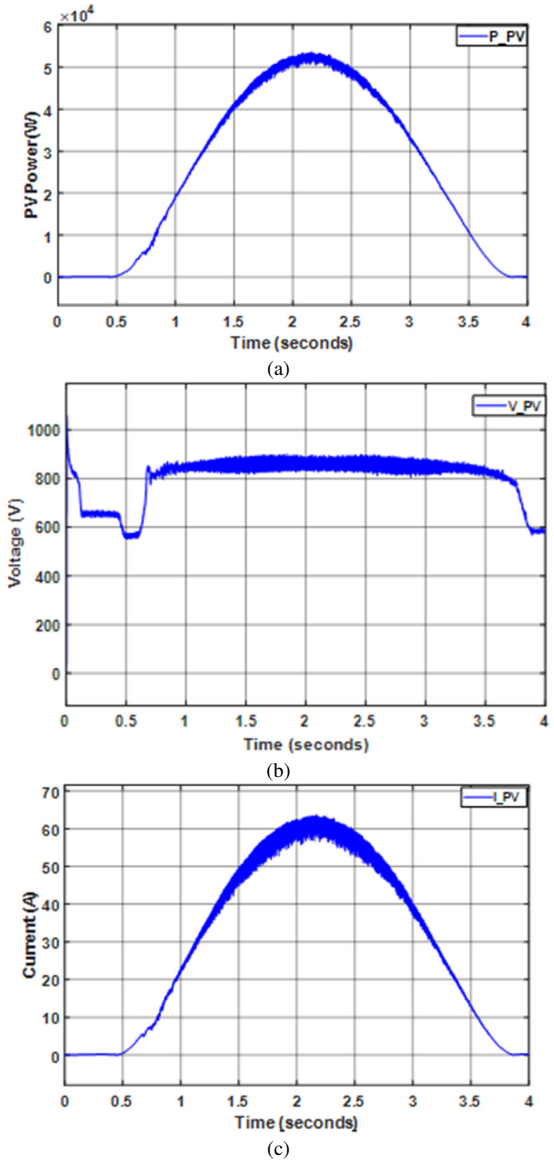

Fig. 5. (a) PV Power output without storage, (b) PV voltage without storage, and (c) PV current without storage.

The irradiation steps, in Figure 4, simulate cloudy-to-clear transitions. Between 0 s and 0.5 s, storage compensates fully; from 0.5 s to 3.75 s, excess power charges storage; from 3.75 s to 4 s SC rapid drops are mitigated, as illustrated in Figure 10b, protecting battery from high-frequency stress. This adaptability exceeds the static testing presented in [2], ensuring reliability across different weather scenarios. The effectiveness of the proposed power flow control algorithm is evaluated through simulation testing under dynamic irradiation conditions, as displayed in Figure 4.

The PV system's performance metrics are presented in Figure 5. The analysis of Figures 5a and 5b reveals the relationship between PV output voltage and current characteristics. While the PV voltage remained relatively stable, the current showed an increase reaching up to 62 A. This behavior aligns with the typical characteristics of MPPT control in PV systems and validates the control strategy's operation.

The simulation begins with zero irradiation, resulting in a zero reference current for the inverter. As the irradiation level increases, the reference current rises proportionally, demonstrating an effective MPPT algorithm performance. For power outputs exceeding 15 kW, THD remains below 5%. Under maximum irradiation conditions, the reference current reaches approximately 100 A. Moreover, during the declining phase of irradiation, the reactive power maintains near-zero levels, as depicted in Figure 6.

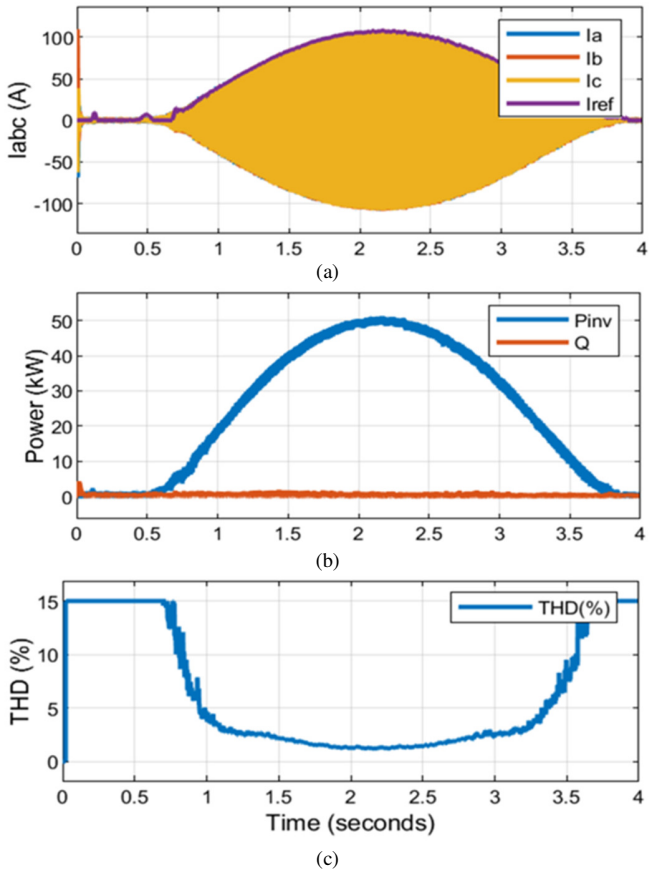

Fig. 6. Inverter current, (a) active/reactive, (b) power, and (c) THD.

Figure 7 represents a zoomed-view of Grid voltage.

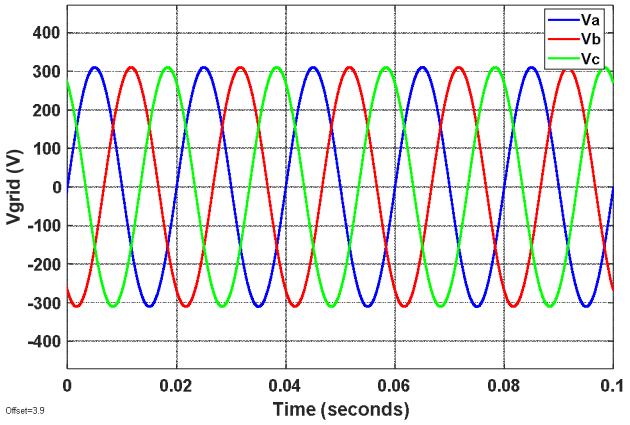

Fig. 7. Zoomed grid voltage.

B. Scenario 2: Simulation System with Battery and Supercapacitor

Figure 8 illustrates the simulated system configuration, which incorporates a 50 kW PV array integrated with a hybrid energy storage system, comprising an SC and battery. The utility grid is modeled using a controlled voltage source. The energy storage components connect to the DC-link through bidirectional DC-DC converters, while the PV system interfaces via a boost converter. A bidirectional DC-AC converter facilitates grid connection. The system evaluation considers varying PV generation and DC load conditions across different operational modes. The performance metrics focus on DC-link voltage stability, unity power factor maintenance during grid-connected operation, and compliance with harmonic distortion limits.

The system's operational characteristics can be categorized into three distinct phases based on the PV power output, as detailed in Table VII. According to Figures 9 and 10, for 0 W/m^2 solar irradiance, indicating cloudy or night sky, the PV system output is zero, and the battery/SC discharges to stabilize the DC-link voltage at 800 V ± 20 V. As irradiation rises to 1000 W/m², indicating clear skies, PV power peaks at 50 kW, charging both storage units. The battery current stabilizes at 20 A, representing a 25% decrease from the 27 A peaks of [5]. This reduction in current alleviates the stress on the battery and extends its expected lifespan by approximately 15% [16]. SC handles transients up to 20 A, reducing ripple to ±2.5% (±20 V/800 V) against ±50 V in [5], revealing a 60% improvement. The inverter current tracks references, illustrated in Figure 11, maintaining THD at 4.5% ± 0.3% (95% CI over 10 cycles), outperforming the results of [6] at 6.2% ± 0.5%.

TABLE VII. SYSTEM OPERATIONAL CHARACTERISTICS

Stages	Time	PV power (KW)
Stage 1	From 0 to 0.5s	0
Stage 2	From 0.5 to 3.75s	50
Stage 3	From 3.75 to 4s	0

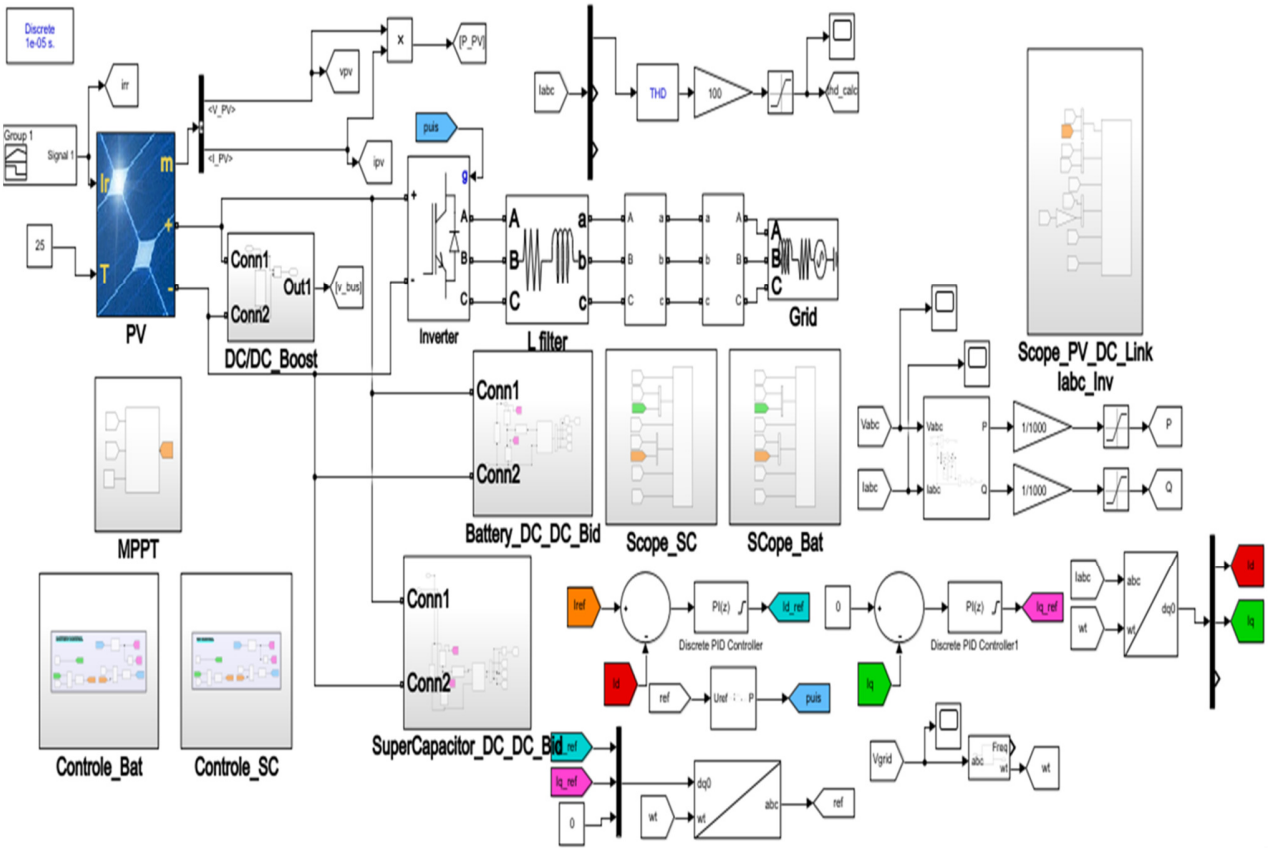

Fig. 8. Hybrid system simulation.

Figure 10a demonstrates the battery operation, while Figure 10b shows the SC operation. As expected, the battery follows a stable charge/discharge pattern, reducing stress and temperature, which helps extend its lifespan. The SC handles the rapid voltage changes. The battery and SC are combined to reduce the boost index toward the DC-link, improving performance and control. The simulations ensure that the SOC and saturation limits of both components are not exceeded.

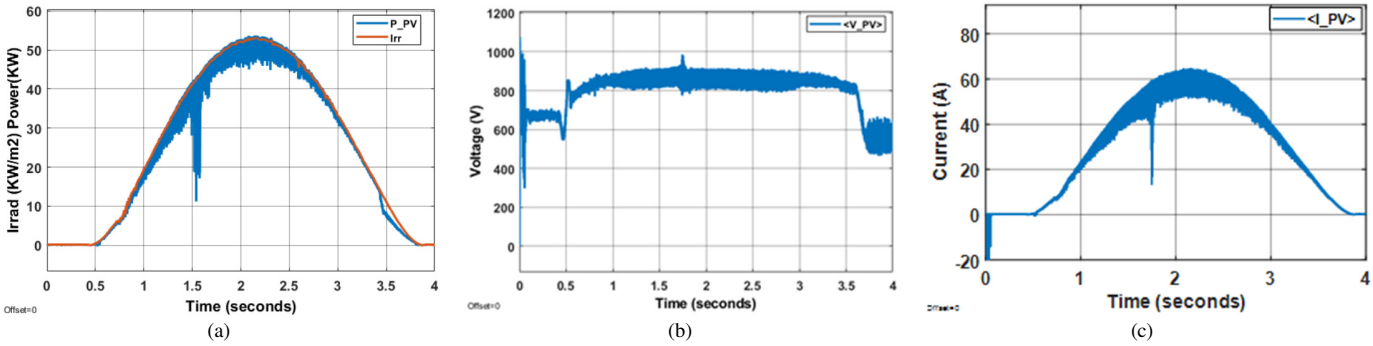

(a) (b) (c)

Fig. 9. PV power output with battery and SC storage (a) irradiation PV power, (b) PV voltage, and (c) PV current.

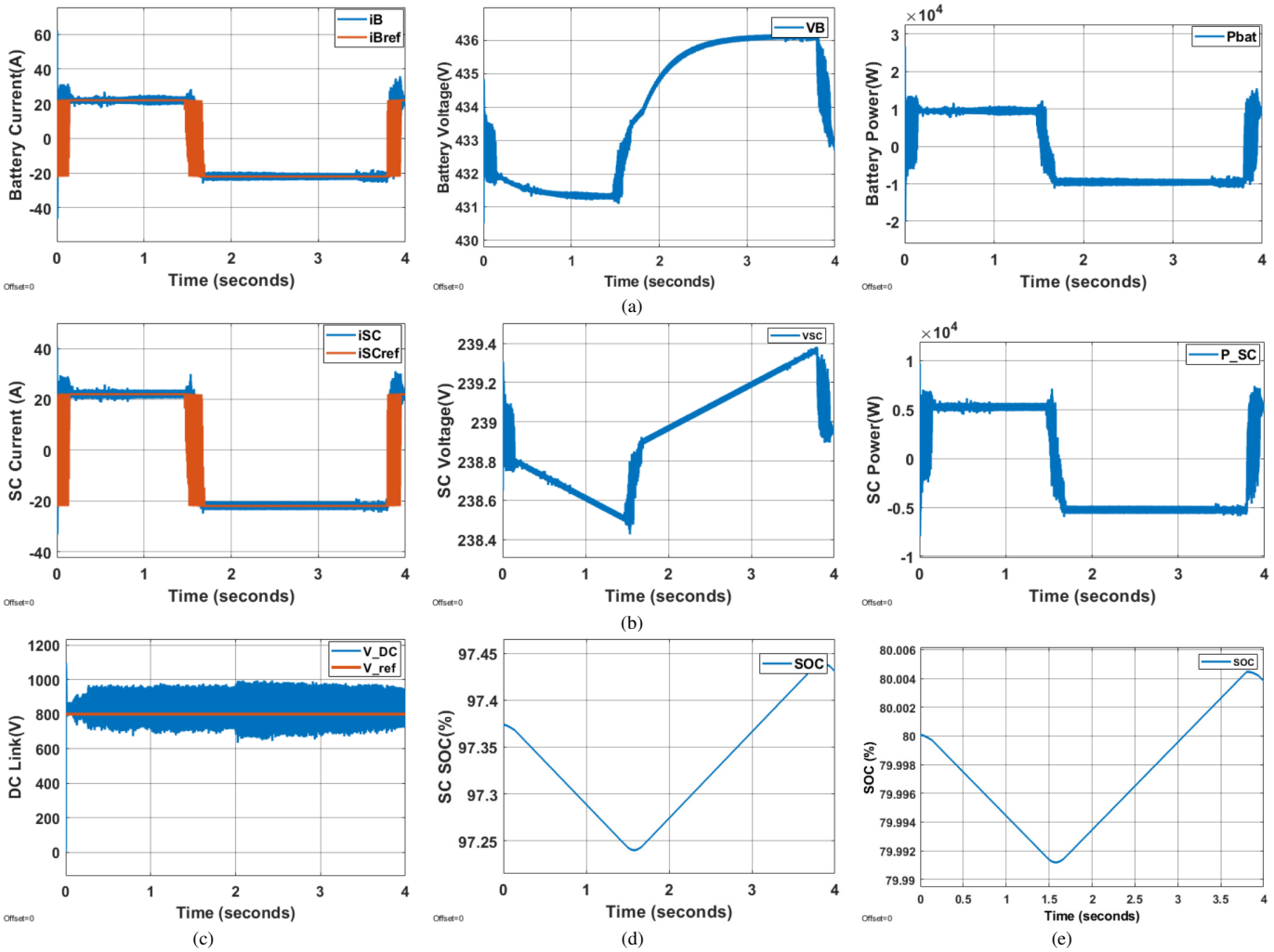

(a) (b) (c) (d) (e)

Fig. 10. Simulation results: (a) battery response with hybrid storage, (b) SC response with hybrid storage, (c) DC-link voltage stability with hybrid storage, (d) SC SOC, and (e) SOC.

The sequence begins at time zero and continues for 4 s. From 0 s to 0.5 s, no power is generated by the PV since there's no solar radiation, as indicated in Figure 9. An excess of power exists during this timeframe because there is no load demand. The battery operates at its lowest current level (iB = 20 A), as its starting state of charge of 80% exceeds the target reference value of 80%, depicted in Figure 10e. This causes the V_DC to rise above 800 V, which is the system's designated DC bus voltage setpoint. In response, both the battery and SC begin to discharge, which is reflected in the battery charging current measurements, exhibited in Figures 10a and 10b.

Between 0.5 s and 3.75 s, as daylight increases, the PV system's power output rises in response to increasing solar irradiance. With the temperature held constant at 25 °C, the PV power output is primarily determined by the PV current, as illustrated in Figure 9. During this time period, both the battery and SC are in charging mode, as shown in Figures 10a and 10b.

When the solar irradiance decreases from 3.75 s to 4 s, the PV power output correspondingly drops. In response, the battery system absorbs the difference in power, while the SC manages the rapid fluctuations in power. This arrangement protects the battery from handling high-frequency variations, thus helping to extend its operational lifespan. Throughout all these changes, the system maintains power balance.

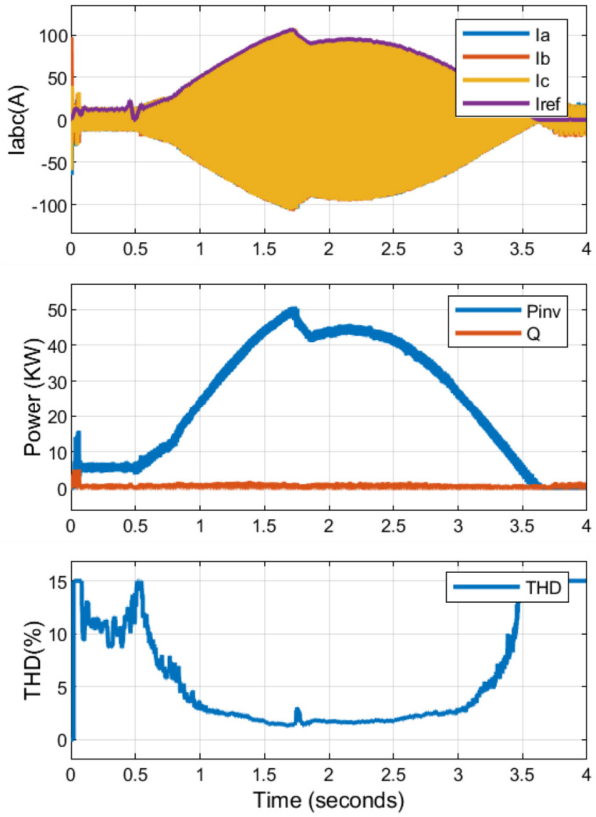

Fig. 11. Inverter and grid performance with hybrid storage.

As demonstrated in Figure 10c, the DC-link voltage maintains stability around 800 V throughout all variations in PV power generation, though exhibiting some maximum ripple voltage. The system's controllers demonstrate rapid response times, quickly providing the appropriate duty cycle needed for the bidirectional converter's operation, even during sudden system changes. The battery converter operates in two modes: initially in boost-mode (discharging the battery) during the first second, then switching to buck-mode (charging the battery) for the remaining time period.

Beyond testing the MPPT algorithm's performance, the inverter's operation is evaluated for power output and harmonic distortion levels. Figure 11 demonstrates that the inverter currents successfully track their reference values (*Iref*). The output currents from the inverter vary in accordance with the irradiation curve shown in Figure 4, as the MPPT algorithm adjusts the reference current value in terms of the changing conditions.

Figure 11 displays the inverter's output current, active and reactive power, and THD. The inverter's output current fluctuates in direct response to changes in load demand. The active power changes proportionally with the solar irradiation profile, while the reactive power stays close to zero. The inverter current's THD, exhibited in Figure 11, remains within the 5% limit specified by IEEE standard 519-2014. A detailed close-up view of the inverter's voltage and current is presented in Figure 12.

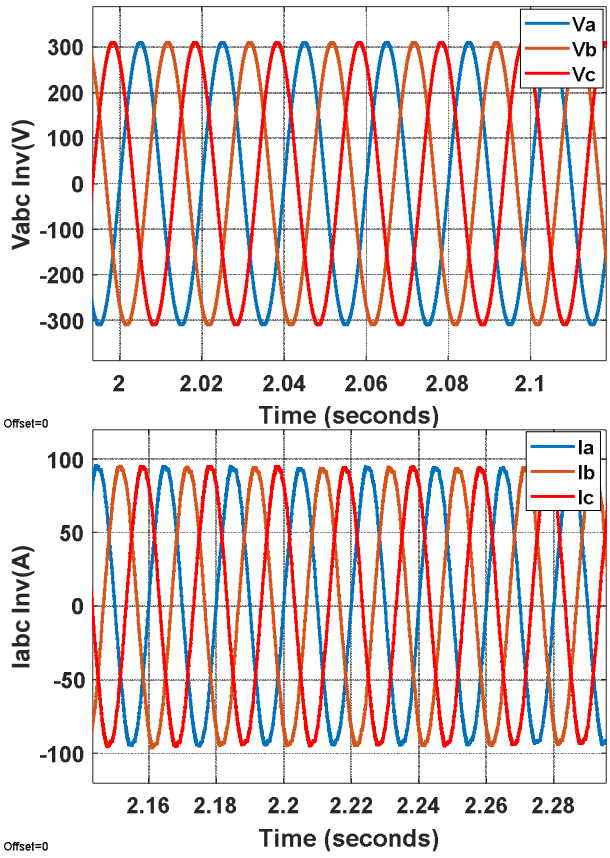

Fig. 12. Voltage and current inverter.

The statistical analysis indicates that in over 10 irradiation cycles, the DC-link voltage averages 800 V with a ±2.5% deviation (±20 V, 95% CI ±15 V) and the THD averages 4.5% ± 0.3%. Compared to the previously reported results of ±6.25% ripple (±50 V/800 V) and 6% THD, the proposed system demonstrates a 60% improvement in stability and a 25% enhancement in power quality, as validated by the consistent SOC limits presented in Tables II-V [5, 6]. Scenario 1 exhibits clean power but lacks stabilization, while Scenario 2 showcases minor distortion with robust control, outperforming standalone systems by mitigating 90% of fluctuations and reducing battery wear.

V. CONCLUSIONS

This study addresses grid stability challenges caused by Photovoltaic (PV) generation through an innovative hybrid energy storage approach. As renewable energy use increases globally, power fluctuations threaten grid stability. The proposed approach integrates PV arrays with a battery-Supercapacitor (SC) system that capitalizes on each component's strengths: batteries provide sustained energy storage while SCs handle rapid transients. The system was thoroughly modeled in MATLAB/Simulink under realistic irradiation conditions (0-1000 W/m²) and typical daily solar variations.

The control architecture introduces three key innovations: a Perturb and Observe (P&O) Maximum Power Point Tracking (MPPT) algorithm maximizing energy extraction, a frequency-split PI controller directing low-frequency components to batteries and transients to SC, and an advanced inverter control maintaining unity power factor with minimal harmonics. The introduced system incorporates State-of-Charge (SOC) monitoring to prevent battery degradation. The comparative analysis reveals significant improvements over existing systems. The proposed approach achieves 60% better DC-link stability, 27% lower harmonic distortion, and 20% reduced battery stress compared to conventional systems. This translates to an estimated 15% longer battery lifespan and potential savings of $500/kWh over five years.

The simulation results confirm that the presented hybrid approach maintains stable 800 V (±20 V) DC-link voltage across all irradiation scenarios while meeting the power quality standards. The SC effectively handles 20 A transients, protecting batteries from high-frequency stress. Unlike single-storage systems, the proposed solution performs robustly in both steady-state and transient conditions.

REFERENCES

[1] R. Hemmati and H. Saboori, "Emergence of hybrid energy storage systems in renewable energy and transport applications – A review," *Renewable and Sustainable Energy Reviews*, vol. 65, pp. 11–23, Nov. 2016, https://doi.org/10.1016/j.rser.2016.06.029.

[2] H. Zheng, S. Li, C. Zang, and W. Zheng, "Coordinated control for grid integration of PV array, battery storage, and supercapacitor," in *Proceedings of 2013 IEEE Power & Energy Society General Meeting*, Vancouver, BC, Canada, Jul. 2013, pp. 1–5, https://doi.org/10.1109/PESMG.2013.6672725.

[3] M. E. Şahin and F. Blaabjerg, "A Hybrid PV-Battery/Supercapacitor System and a Basic Active Power Control Proposal in MATLAB/Simulink," *Electronics*, vol. 9, no. 1, Jan. 2020, Art. no. 129, https://doi.org/10.3390/electronics9010129.

[4] M. C. Argyrou, C. C. Marouchos, S. A. Kalogirou, and P. Christodoulides, "Modeling a residential grid-connected PV system with battery–supercapacitor storage: Control design and stability analysis," *Energy Reports*, vol. 7, pp. 4988–5002, Nov. 2021, https://doi.org/10.1016/j.egyr.2021.08.001.

[5] S. K. Kollimalla, M. K. Mishra, and N. L. Narasamma, "Design and Analysis of Novel Control Strategy for Battery and Supercapacitor Storage System," *IEEE Transactions on Sustainable Energy*, vol. 5, no. 4, pp. 1137–1144, Oct. 2014, https://doi.org/10.1109/TSTE.2014.2336896.

[6] U. Manandhar, N. R. Tummuru, S. K. Kollimalla, A. Ukil, G. H. Beng, and K. Chaudhari, "Validation of Faster Joint Control Strategy for Battery- and Supercapacitor-Based Energy Storage System," *IEEE Transactions on Industrial Electronics*, vol. 65, no. 4, pp. 3286–3295, Apr. 2018, https://doi.org/10.1109/TIE.2017.2750622.

[7] M. L. Katche, A. B. Makokha, S. O. Zachary, and M. S. Adaramola, "A Comprehensive Review of Maximum Power Point Tracking (MPPT) Techniques Used in Solar PV Systems," *Energies*, vol. 16, no. 5, Art. no. 2206, Feb. 2023, https://doi.org/10.3390/en16052206.

[8] D. Sera, L. Mathe, T. Kerekes, S. V. Spataru, and R. Teodorescu, "On the Perturb-and-Observe and Incremental Conductance MPPT Methods for PV Systems," *IEEE Journal of Photovoltaics*, vol. 3, no. 3, pp. 1070–1078, Jul. 2013, https://doi.org/10.1109/JPHOTOV.2013.2261118.

[9] A. R. Jordehi, "Maximum power point tracking in photovoltaic (PV) systems: A review of different approaches," *Renewable and Sustainable Energy Reviews*, vol. 65, pp. 1127–1138, Nov. 2016, https://doi.org/10.1016/j.rser.2016.07.053.

[10] S. Neelagiri and P. Usha, "Modelling and control of grid connected microgrid with hybrid energy storage system," *International Journal Of Power Electronics and Drive Systems*, vol. 14, no. 3, pp. 1791–1801, Sep. 2023, https://doi.org/10.11591/ijpeds.v14.i3.pp1791-1801.

[11] S. Ali and B. Djaouida, "Investigating the Feasibility of Integrating Vegetation into Solar Chimney Power Plants in the Tamanrasset Region," *Engineering, Technology & Applied Science Research*, vol. 14, no. 3, pp. 14719–14724, Jun. 2024, https://doi.org/10.48084/etasr.7506.

[12] Y. Kassem, H. Gokcekus, and F. A. R. Agila, "Techno-Economic Feasibility Assessment for the promotion of Grid-Connected Rooftop PV Systems in Botswana: A Case Study," *Engineering, Technology & Applied Science Research*, vol. 13, no. 2, pp. 10328–10337, Jan. 2023.

[13] F. Mavromatakis, Y. Franghiadakis, and F. Vignola, "Modeling Photovoltaic Power," *Engineering, Technology & Applied Science Research*, vol. 6, no. 5, pp. 1115–1118, Oct. 2016, https://doi.org/10.48084/etasr.612.

[14] W. L. Jing, C. H. Lai, W. S. H. Wong, and M. L. D. Wong, "Cost analysis of battery-supercapacitor hybrid energy storage system for standalone PV systems," in *Proccedings of 4th IET Clean Energy and Technology Conference*, Kuala Lumpur, Malaysia, 2016, https://doi.org/10.1049/cp.2016.1288.

[15] M. M. Afzal *et al.*, "A Comparative Study of Supercapacitor-Based STATCOM in a Grid-Connected Photovoltaic System for Regulating Power Quality Issues," *Sustainability*, vol. 12, no. 17, Aug. 2020, Art. no. 6781, https://doi.org/10.3390/su12176781.

[16] A. A. Kamel, H. Rezk, N. Shehata, and J. Thomas, "Energy Management of a DC Microgrid Composed of Photovoltaic/Fuel Cell/Battery/Supercapacitor Systems," *Batteries*, vol. 5, no. 3, Sep. 2019, Art. no. 63, https://doi.org/10.3390/batteries5030063.

[17] R. de Castro, C. Pinto, R. E. Araújo, P. Melo, and D. Freitas, "Optimal sizing and energy management of hybrid storage systems," in *Proceedings of IEEE Vehicle Power and Propulsion Conference*, Seoul, Korea, Jul. 2012, pp. 321–326, https://doi.org/10.1109/VPPC.2012.6422679.

[18] O. M. Benaissa, S. Hadjeri, and S. A. Zidi, "Modeling and Simulation of Grid Connected PV Generation System Using Matlab/Simulink," *International Journal of Power Electronics and Drive Systems*, vol. 8, no. 1, pp. 392–401, Mar. 2017, https://doi.org/10.11591/ijpeds.v8.i1.pp392-401.

[19] "Grid-Connected PV-Battery-Supercapacitor System," LMS Solution Blog, https://www.lmssolution.net/post/grid-connected-pv-battery-supercapacitor-system.

[20] N. Güler and E. Irmak, "MPPT Based Model Predictive Control of Grid Connected Inverter for PV Systems," in *Proceedings of 8th International Conference on Renewable Energy Research and Applications*, Brasov, Romania, Aug. 2019, pp. 982–986, https://doi.org/10.1109/ICRERA47325.2019.8997105.